Radiation Induced Grafting of Glycidylmethacrelate onto Polypropylene Films for Removal of Mercury from Aqueous Solutions

Nabila A. Maziad[a]; Samia A. Abo-Farha[b]; Laila F. M. Ismail[b]

[a] National Center for Radiation Research and Technology, Nasser City, Cairo, Egypt [b] Chemistry Department, Faculty of Science, Al-Azhar University, Nasser City, Cairo, Egypt

PLEASE SCROLL DOWN FOR ARTICLE

Taylor & Francis
Taylor & Francis Group

Radiation Induced Grafting of Glycidylmethacrelate onto Polypropylene Films for Removal of Mercury from Aqueous Solutions

NABILA A. MAZIAD[1,*], SAMIA A. ABO-FARHA[2] and LAILA F. M. ISMAIL[2]

[1]*National Center for Radiation Research and Technology, Nasser City, Cairo, Egypt.*
[2]*Chemistry Department, Faculty of Science, Al-Azhar University, Nasser City, Cairo, Egypt.*

This work illustrates the modification of polypropylene (PP) films through its grafting with glycidylmethacrelate monomer (GMA). Further chemical treatment of PP-g- GMA to convert epoxy groups into amine groups is discussed. Different factors affecting the grafting percent such as solvents, monomer concentrations, irradiation dose have been studied. Fourier transform infrared (FTIR) and thermogravimetric (TGA) analysis confirm the grafting of PP. Morphological changes of PP, PP-g-GMA and treated PP-g-GMA are confirmed by scanning electron microscopy (SEM). The X-ray diffraction (XRD) pattern shows changes in the crystallinity on grafting. Adsorption and kinetic studies of mercury onto the prepared PP grafted and chemically treated films in sorption of Hg^{+2} metal ions from aqueous solutions have been studied. The experimental data fit favorably to the Langmuir isotherm with a high correlation coefficient. Moreover, the pseudo first and second order kinetics is also indicated. The results suggest that the pseudo-second-order kinetic model better represent the adsorption kinetics, suggesting that the adsorption process may be chemisorptions. It is more likely to predict that the adsorption behavior may involve valence forces through the sharing of electrons between Hg^{2+} and adsorbent. On the basis of these investigations, the applicability of the prepared membranes is discussed. Also the confirmation of metal ions adsorbed was confirmed using EDS spectrometric techniques.

Keywords: Glycidylmethacrylate, radiation grafting, adsorption isotherm, kinetic studies

1 Introduction

Mercury is a pervasive contaminant that is highly toxic and readily accumulated by organisms. Even if present in traces, its high toxicity makes it an environmental threat in industrial, mining, and domestic wastes (1–3). The major effects of mercury poisoning are neurological and renal disturbances, as well as impairment of pulmonary function (4–6).

Since heavy metal ions are not biodegradable, they are usually removed physically or chemically from the contaminated water. Conventional methods that have been used to remove heavy metal ions from various industrial effluents usually include chemical precipitation, membrane separation, ion exchange, evaporation, and electrolysis, etc. and are often costly or ineffective, especially in removing heavy metal ions from dilute solutions (7–9). Adsorption appears to be a good alternative for the treatment of effluents (10, 11).

Grafting copolymerization reaction is usually performed either chemically (13), photochemically (13) or by a radiation technique (14, 15). The last was found to be the most promising method, and the effect of solvent nature on the extent of grafting by radiation grafting was found to be important (12, 16–18). A direct radiation grafting method and simultaneous irradiation in the presence of monomer, polymer and solvent results in the creation of active centers, peroxides or free radicals, depending on the conditions of irradiation. The grafting can occur throughout the bulk materials or in superficial layers of a desirable thickness. The preparation of adsorbents for metal ions by radiation-induced grafting has also been reported (19).

Modification of PP through a grafting technique with reactive monomers is considered to be one of the main routes to overcome these problems (13), as will as the hydrophobic nature of polypropylene (PP), and the absence of any reactive functional groups in its molecular structure, its use in certain applications, especially in fiber manufacture.

The present study is an attempt to illustrate the modification of PP through its grafting with glycidylmethacrelate (GMA). The study was extended to the characterization of the grafted films taking into consideration the main

*Address correspondence to: Nabila A. Maziad, National Center for Radiation Research and Technology, Nasser City, Cairo, Egypt. E-mail: nabila@yahoo.com

physical and chemical properties and the uptake of the modified films. Moreover, the effect of various experimental conditions on the adsorption of Hg^{2+} on the prepared films such as the effect of pH, initial metal ion concentration, adsorption isotherms and also the adsorption kinetics were studied.

2 Experimental

2.1 Materials

Polypropylene (PP) films of thickness 0.07 mm were supplied by Mesr Packing Company, Egypt, Glycidylmethacrelate purity 99% ($CH_2C(CH_3)COOCH_2$ $CHOCH_2$, GMA, Aldrich), trimethylamine ($N(CH_3)_3$, TMA, Aldrich), hydroxylamine (HA, Aldrich), diethanolamine (DEA, Aldrich), and tri(hydroxymethyl) aminomethane ($HOCH_2)_3CNH_2$, THMAM, Aldrich) were used without further purification. All other chemicals of reagent grade were used without further purification.

2.2 Graft Copolymerization

Strips of PP films were washed with acetone, dried at 50°C in a vacuum oven, weighed and immersed in different GMA monomer solution with Dichloroethane solvent and Fe Cl_3 inhibitor of 2–2.5 wt% in a glass ampoules bubbled N_2 gas atmosphere and then subjected to ^{60}Co- γ- rays at a dose rate from 0.49 to 1.50 Gy/s. The grafted films were removed and washed thoroughly with acetone followed by distilled hot water to extract the residual monomer and the homopolymer which may be accumulated in the film. The films were dried in vacuum oven at 50–60°C for 24 h and weighed.

The degree of grafting was calculated as the percentage increase in the weight as follows (20).

$$Degree\ of\ grafting\,(\%) = ((W_g - W_0)/W_0) \times 100$$

where W_0 and W_g represent the weights of initial and grafted films, respectively.

2.3 Chemical Treatment of Graft Copolymers

Epoxy group of GMA-grafted PP films was converted into hydroxylamine groups by soaking GMA-grafted PP films in hydroxylamine solution. The treatment was carried out in a reflux system to improve the functionality of the prepared grafted films, the epoxy groups formed of GMA can be allowed to be introduced by various functional groups, such as amines (21, 22).

2.4 Swelling Measurement

The clean dried grafted and treated film of known weights were immersed in distilled water at 25°C until the equilibrium was reached (24 h). The films were removed, quickly and just dried on the surface from water with absorbent paper and then weighed.

$$Water\ up\ take\,(\%) = ((W_s - W_g)/W_g) \times 100$$

where W_s and W_g represents the weights of the wet and dry grafted films, respectively (20).

2.5 FTIR Spectroscopy

FTIR measurement carried out using (Perkin–Elmer) 1430 Ratio Recording Infrared Spectrophotometer, England, in the range from 4000–5000 cm^{-1}.

2.6 Thermal Gravimetric Analysis (TGA)

Shimadzu (TGE) instrument of type (TGA–4000) was used for measurement of (TGA). In the present study, nitrogen flow was kept at a constant rate of about 10°C/min to prevent thermal oxidation processes of polymer sample.

2.7 Scanning Electron Microscope (SEM)

The surface topography of the grafted films was studied using (JEOL SEM–25) scanning electron microscope. Prior to examination, the grafted films were dried under sputter coated gold. Also, the metal ion dispersion and morphology of chelating copolymer particles were recorded by scanning electron microscopy (SEM; JEOL-JSM-5400 Scanning Electron Microscope, Japan), with an energy dispersive spectroscopy (EDS)

X-ray spectrometer (23).

2.8 X-Ray Diffraction (XRD)

X-ray diffraction patterns of the polymer films were measured with a modern (Shimadzu Diffractometer xD-D$_1$ series) which is operated fully automatically. The X- ray copper target tube was operated at 40 KV and 30 mA and all the diffraction patterns were examined at room temperature and under constant operating conditions.

3 Results and Discussion

3.1 Optimum Grafting Conditions

3.1.1. *Effect of solvent on the degree of grafting*

Solvents are basically used in radiation grafting experiments to enhance the degree of accessibility (20) of monomers for grafting sites within the polymers. Figure 1 shows the variation of the grafting percent of GMA onto PP at different solvents. It represents the fact that the higher degree of grafting is obtained in the presence of benzene if it is compared with the other solvents. The maximum grafting occurs in benzene, but the samples were rigid and
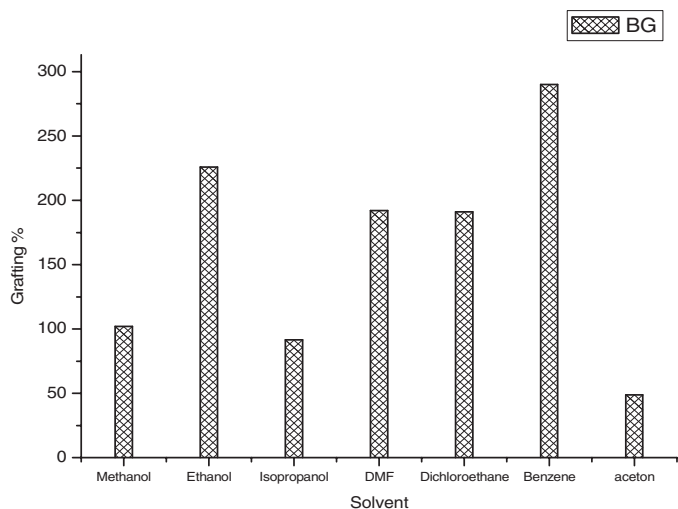
Fig. 1. Effect of solvent on the degree of grafting of glycidyl-methacrelate (GMA) onto polypropylene (PP), FeCl$_3$ is used as inhibitor at irradiation dose 20 kGy.

crunchable, while, a reasonable transparent and flexible film was obtained when dichloromethane solvent was used.

3.1.2. *Effect of monomer concentration on the degree of grafting*

Figure 2 represents the variation of (GMA) monomer concentration on the degree of grafting of PP. It shows a sharp increase in the degree of grafting with increasing monomer concentration up to 60 wt% and reaches a near saturation level when the monomer concentration increases. These results can be explained that the high monomer concentration produces a great number of the free radicals formed and
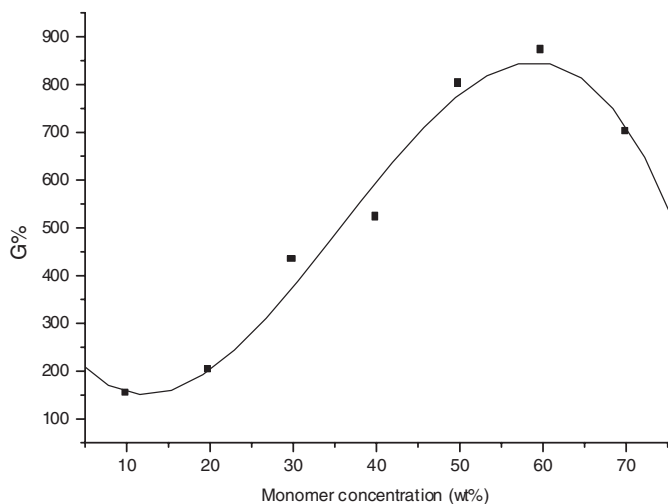

Fig. 2. Effect of monomer concentration on the degree of grafting of glycidylmethacrelate (GMA) onto polypropylene (PP), FeCl$_3$ is used as inhibitor at irradiation dose 20 kGy and dichloroethane as a solvent.

Fig. 3. Effect of irradiation dose on the degree of grafting of glycidylmethacrelate (GMA) onto polypropylene (PP), FeCl$_3$ is used as inhibitor at irradiation dose 20 kGy and dichloroethane as a solvent.
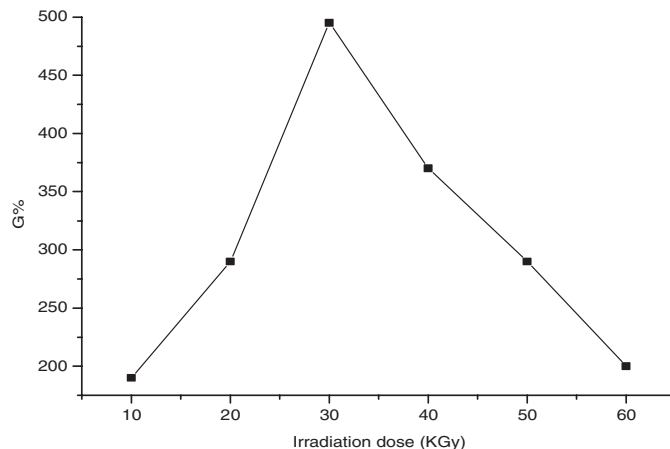
crosslinked in the backbone of the polymer chain. Further increase in the monomer concentration more than 60 wt% leads to a slight decrease in the amount of graft which may be attributed to the increase in the viscosity of the reaction mixture at the later stages of polymerization. This may hinder the diffusion of monomer towards the polymeric matrix and consequently, the net result is a lower graft percentage when the total monomer concentration exceeds the optimum condition (12, 20).

3.1.3. *Effect of irradiation dose on the degree of grafting*

The irradiation dose is an important factor in radiation grafting copolymerization process. In the direct radiation method, the total dose determines the number of active sites able to be copolymerized (20). Therefore, the effect of irradiation dose on the grafting yield of GMA onto PP films was investigated as shown in Figure 3. Results show that, initially, the degree of grafting increases with increasing irradiation dose due to the increase in radical concentration; thereafter, it tends to level off due to the formation of homopolymer which restricts the diffusivity of monomer through the surface of PP polymer (20).

3.2 Characterization of Grafted Membranes

3.2.1. *Swelling behavior*

It is very important that the grafted membranes exhibit suitable hydrophilic properties due to the grafting of hydrophilic monomer such as glycidylmethacrelate onto the polymeric substrate. Figure 4 shows the percentage water uptake as a function of degree of grafting for PP-g-GMA films before and after treatment. It can be seen that the percentage water uptake increases as the percentage grafting increases for grafted and treated membranes. This is due to the hydrophilicity of polyglycidylmethacrelate chains
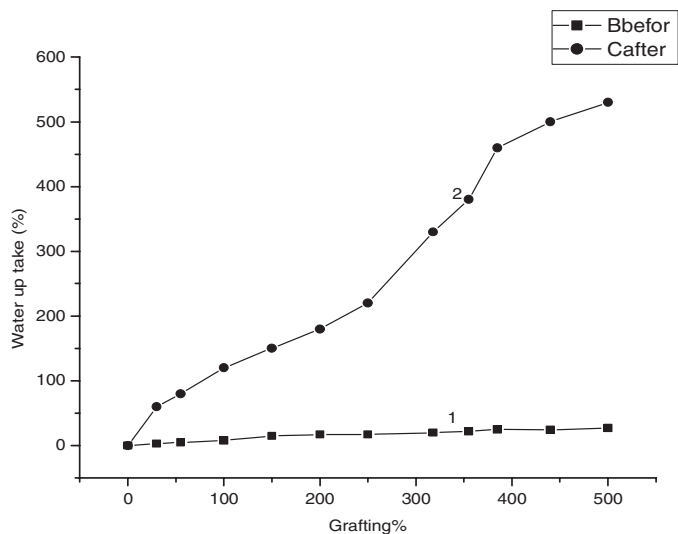
Fig. 4. Percentage water uptake for untreated (curve 1) and treated (curve 2) PP-g-GMA.

Fig. 5. FTIR spectrum of PP-GMA using different degree of grafting.

grafted onto PP films. and their solubility in water in its free state (24). This increase of water uptake in the case of treated grafted membranes may be attributed to the conversion of epoxy groups into amine groups which in turn, improves the swelling behavior of the grafted treated membranes.

3.2.2. *FTIR spectrum*

Infrared spectra of PP, PP-g-GMA with a different degree of grafting are illustrated in Figure 5. In addition to the characteristic bands of PP (the band at 2700–3000 cm^{-1} is due to the −CH stretching vibration band of −CH group of PP, three new absorption peaks were observed in the spectrum of the copolymer. The new peak at 1740- and 1240 cm^{-1} (C=O stretch and C−O stretch) of acetate group, and 700, 850, 910 cm^{-1} are bending vibrations. The appearance of the new peaks in the spectrum of PP-g-GMA clearly demonstrated that GMA has been successfully grafted onto PP films (25).

3.2.3. *Thermal gravimetric analysis (TGA)*

Thermogravimetric analysis showed the extent of thermal decomposition for the prepared graft copolymers. It was found that there is a thermal stability till 300°C, after that the sample mass decreased linearly with increase in temperature when the fixed heating rate was fixed at 10°C min^{-1}. The TGA results of blank PP and PP-g-GMA at grafting percent 181% and 244% and the corresponding chemically treated are given in Figure 6. The thermal decomposition of such graft copolymers is characterized by three distinct ranges of decomposition, the range at which the sample is heated from room temperature for blank pp and to 230 and 300 for PP-g-GMA, this may be due to elimination of the moisture absorbed on the grafted side chain. The second range is observed in the temperature rang 300–380 and

from 230–270°C for blank PP and PP-g-GMA films and this may be due to the extensive degradation of the grafted side chains. The third range of degradation occurs from 320 to 500 and 380°C–500°C for PP blank and grafted PP films, respectively, this with a considerable decreasing in weight loss percent of grafted films (26). The thermal degradation

Fig. 6. TGA thermogram for PP-g-GMA at different graft %.

Fig. 7. XRD thermogram of PP-g-GMA using different degree of grafting.

of PP blank is higher than that of the grafted one. However, the grafted films decrease the thermal stability and lower the percentage weight loss of the grafted films.

3.2.4. *X-ray diffraction studies*

X-ray diffraction is the most powerful technique available for the examination of the crystalline or ordered polymers. The degree at which the crystals are oriented parallel to each oth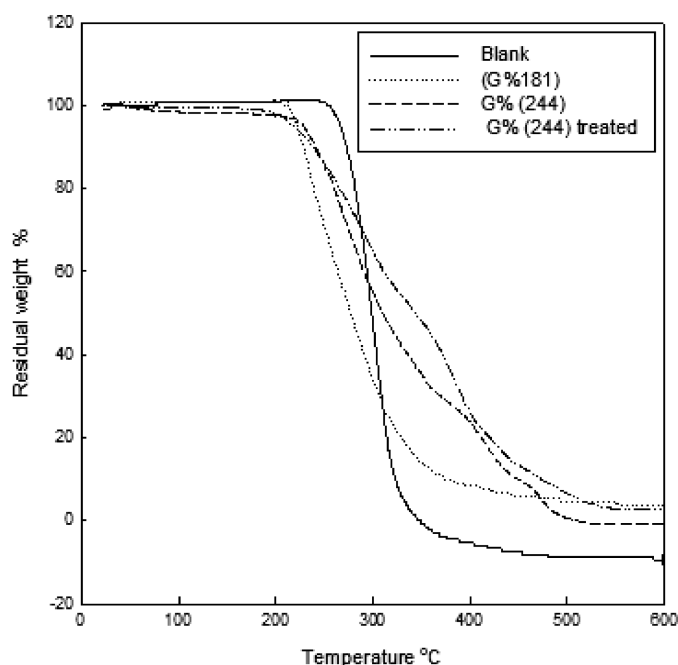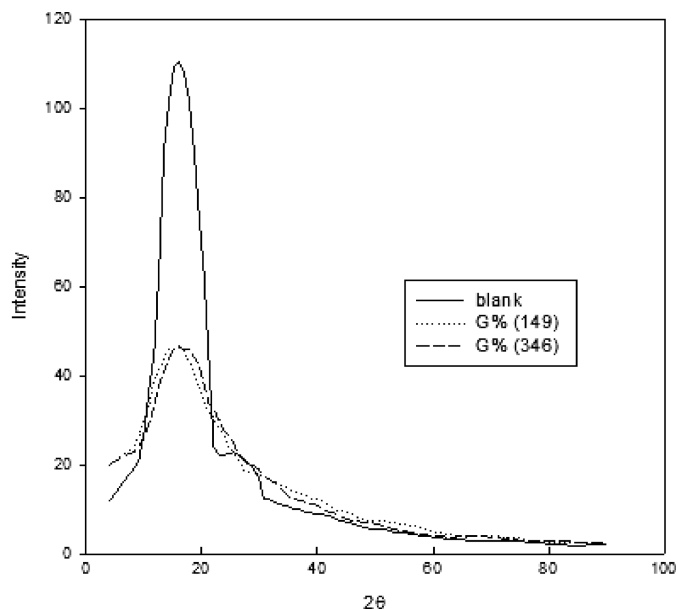er can be driven from the shape and size of the individual selections crystalline material will diffract X-rays at specific angels. The crystalline present in a polymer sample diffract X-ray beams from parallel planes to incident angle θ, which are determined by the Bragg equation:

$$n\lambda = 2d \sin\theta$$

Where λ is the wave length of the beam radiation, d is the distance between the parallel plans in the crystals, n is the angle of incident rays on plane. Figure (8) shows an X-ray diffractogram of blank PP and PP-g-GMA with different grafting percent. It is clear that the incorporation of PGMA chains on the PP films leads to change in its crystalline structure. As the grafting percent increases, the intensity of the crystalline peak decreases and becomes broader which mean that the grafting was occurred on the amorphous and crystalline region and therefore, changes the chain ordered. Consequently, the molecules can rearrange segments to become in a partially crystalline phase again.

3.2.5. *Scanning electron microscopy (SEM)*

Figure 8 shows the SEM micrographs of the surfaces of PP films before (a) and after (b and c) grafting with GMA.

The results clearly show the direct relationship between the grafted and ungrafted on the surface of PP films. After the grafting of PP films (Figure b and c), white particles appeared on the surface. With the treated PP-g-GMA, the surface was spread with a white layer. Moreover, the results reveal that the grafted polymer is chemically bonded to the surface of PP films as the grafted species were found to be unextractable with hot water (13).

The PP-g-GMA before and after treatment were treated with Hg^{2+} (Figure d and e). The results reveal the increase in the amount of Hg^{2+} adsorbed on the surface of the treated films. This indicates the improvement of adsorption of Hg^{2+} after treatment. This can be attributed to the functionality of the formed group after treatment and their ability for absorbing Hg^{2+} ions.

3.3 Adsorption Studies of Hg^{2+} Ions onto PP-g-GMA

3.3.1. *Optimum adsorption conditions*

Adsorption equilibrium is governed by several operational factors, namely, the nature of solute and adsorbent, as well as the pH of the medium, concentration and contact time. Optimization of such operational parameters is the first step toward the understanding of the process (27). In order to determine optimum adsorption conditions, the effect of pH, initial Hg^{2+} concentration and contact time are investigated.

3.3.2. *Effect of pH*

Initial pH value of solution is one of the most important factors influencing the adsorption. Figure 9 shows the effect of pH on adsorption capacity of Hg^{2+} onto PP-g-GMA before and after treatment at different initial pHs for the Hg^{2+} solution concentration of 0.04 mM at 25°C and ionic strength of 0.1 M KNO_3. The amount of adsorption per unit mass of the PP-g-GMA before and after treatment was evaluated by using the following equation:

$$q_e = ((C_0 - C_e)V/W \tag{1}$$

Where, q_e represents the adsorbed Hg^{2+} per unit mass of PP-g-GMA before and after treatment at equilibrium (mM /g), C_0 and C_e are the concentration of Hg^{2+} in the initial solution and in aqueous phase at equilibrium, respectively (mM/l), V is the volume of the aqueous phase (ml) and W is the amount of dry PP-g-GMA films before and after treatment used in grams.

As seen in Figure 9, maximum adsorption capacity was observed at pH 3.5 and 5.0 for PP-g-GMA before and after treatment, respectively. Above pH 3.5 and 5.0 for PP-g-GMA before and after treatment adsorption capacity decreases. Uptake of Hg^{2+} at acidic conditions (pH 3.5 and 5 for Hg^{2+} onto PP-g-GMA before and after treatment, respectively) may be explained as proceeding via complex formation between the metal ions and the function groups
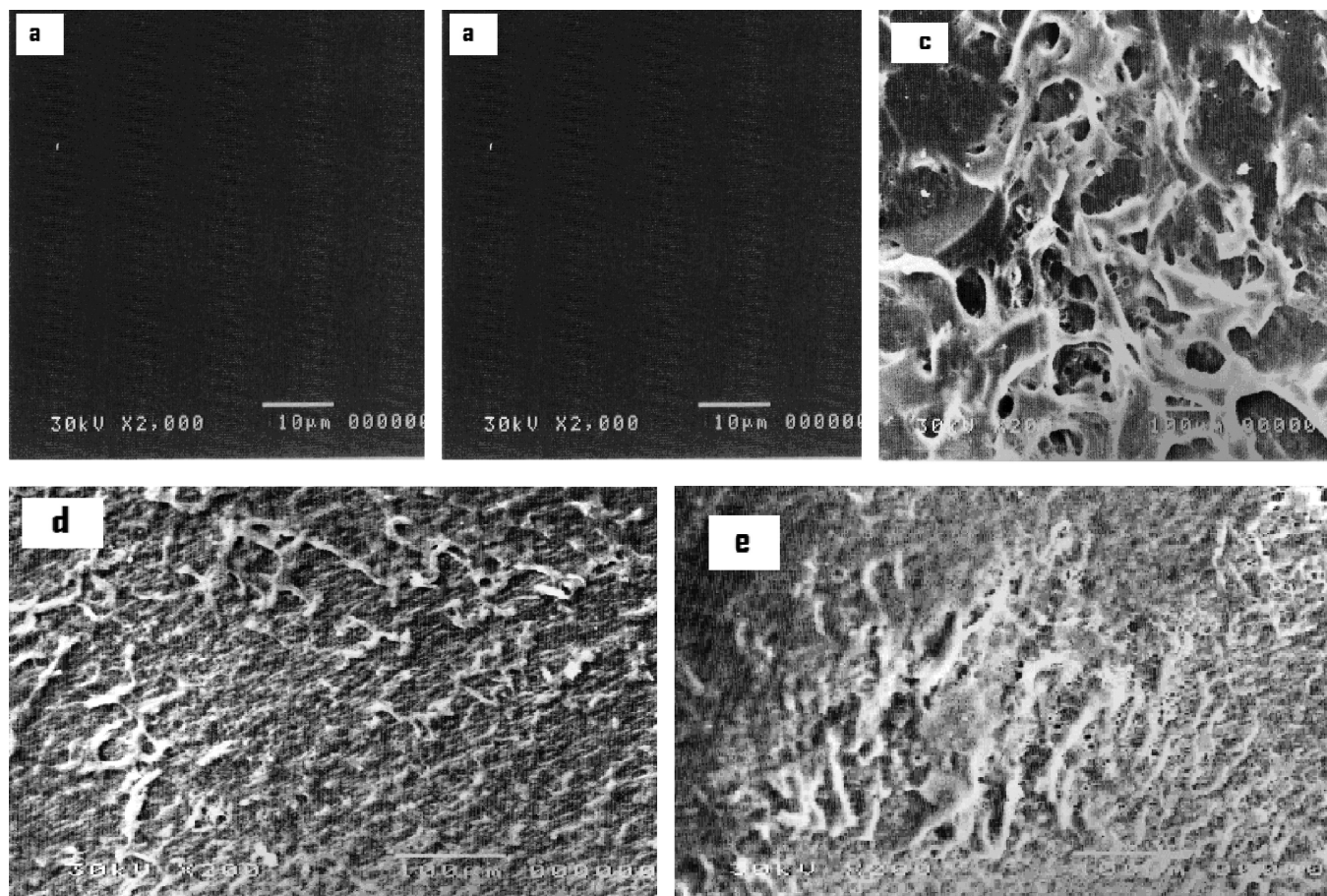
Fig. 8. SEM photograph of: a) ungrafted PP, b) grafted, c) treated, d) grafted doped with Hg^{2+} and e) treated doped with Hg^{2+}.

(28) on PP-g-GMA. As the pH decreases, the active sites become protonated and their ability for the interaction with Hg^{2+} decreases. At pH> 5, the abrupt rise in the uptake of Hg^{2+} may be due to the formation of colloidal precipitates of mercury hydroxide (29).

3.3.3. *Effect of Hg^{2+} concentration*

The effect of initial concentration on the Hg^{2+} adsorption onto PP-g-GMA before and after treatment was investigated in the range of 0.001–0.3 mM of initial Hg^{2+} ions concentrations at pH 4 and 5.0, respectively. Figure 10 shows that the adsorption capacity was concentration dependent and increased with initial concentration of the Hg^{2+} and reaches a near saturation level when the Hg^{2+} concentration increases. An increase in the initial Hg^{2+} concentration led to an increase in the amount of Hg^{2+} adsorbed onto PP-g-GMA. This may be a result of an increase in the driving force of the concentration gradient with the increase in the initial Hg^{2+} concentration (30). This indicated that the initial Hg^{2+} concentration plays an important role in the adsorption capacity of Hg^{2+} onto PP-g-GMA.

3.3.4. *The effect of contact time on the adsorption of Hg^{2+} onto PP-g-GMA.*

Figure 11 shows the uptake of Hg^{2+} onto the PP-g-GMA surface before and after treatment as a function of conditioning time at 25°C and pH 4 and 5.0, respectively. Clearly, a rapid uptake for Hg^{2+} was noticed within the initial 200 and 140 min for PP-g-GMA before and after treatment, respectively above which the adsorption remains constant. The rapid uptake of Hg^{2+} may indicate that most of active sites of the membrane are exposed for the interaction with the metal ions. Moreover, both untreated and treated PP-g-GMA showed high affinity towards Hg^{2+}. This may be due to the fact that Hg^{2+} is a soft acid which has a high affinity towards soft bases such as O atom (31).

3.4 Adsorption isotherm

Adsorption data explain the performance of adsorbent and adsorption isotherms will describe the equilibrium distribution of solute between adsorbent and solution, which will provide the ability to estimate the adsorbent efficiency. Two most common isotherm equations namely, Langmuir, and
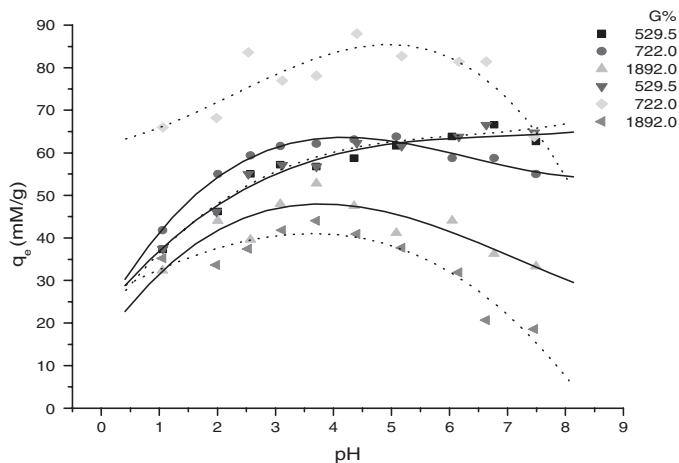
Fig. 9. Effect of pH on adsorption capacity of Hg^{2+} onto PP-g-GMA before (—) and after (. . . .) treatment at various grafting dose and at different initial solution pH. Adsorption conditions: Hg^{2+} concentration: 0.04 mM and I: 0.1 M KNO_3 at 25°C.

Freundlich (32, 33) were tested in this work. The Langmuir equation can be written as follows (34–36).

$$q_e = (Q_0 K_L C_e)/(1 + K_L C_e) \qquad (2)$$

Where q_e is equal to the quantity of dye adsorbed in mM / gram of hydrogel, Q_0 is the maximum adsorption capacity, K_L is the constant of the Langmuir adsorption, and C_e is the equilibrium concentration of Hg^{2+} (mM/l) solution.

Table 1. Linear transformations of the Langmuir isotherm.

Linear Regression	*Plot*	*Parameters*
I $1/q_e = 1/Q_0 + (1/K_L Q_0 C_e)$	$1/q_e$ vs. $1/C_e$	K_L = intercept/slope Q_0 = 1/intercept
II $C_e/q_e = 1/KQ_0 + C_e/Q_0$	C_e/q_e vs. C_e	K_L = slope/intercept Q_0 = 1/ slope
III $q_e = Q_0 - (1/K_L).(q_e/C_e)$	q_e vs. q_e/C_e	K_L = −1/slope Q_0 = intercept
IV $q_e/C_e = KQ_0 - K_L q_e$	q_e/C_e vs. q_e	K_L = −slope Q_0 = intercept/slope

Langmuir adsorption parameters are determined by transforming the Langmuir equation (Equation 1) isotherm to a linear form. The isotherm can be made linear in at least four different ways (37, 38). Depending on the linearizations chosen shown in Table 1, different estimates are obtained for the values of the parameters. This occurs because, depending on the way the isotherm is linearized, and the error distribution changes either for better or for worse (38). The best treatment is obtained by using Equation 1 in Table 1, since this choice tends to minimize deviations from the fitted equation, resulting in the best error distribution. Figure 12 illustrates the linearizations selected to calculate the adsorption parameters of adsorption of Hg^{2+} onto PP-g-GMA before and after treatment.

However, the essential characteristic of the Langmuir isotherm can be expressed by the dimensionless parameter, R_L, called the equilibrium parameter, which can be beneficially used to predict whether a sorption system is favorable
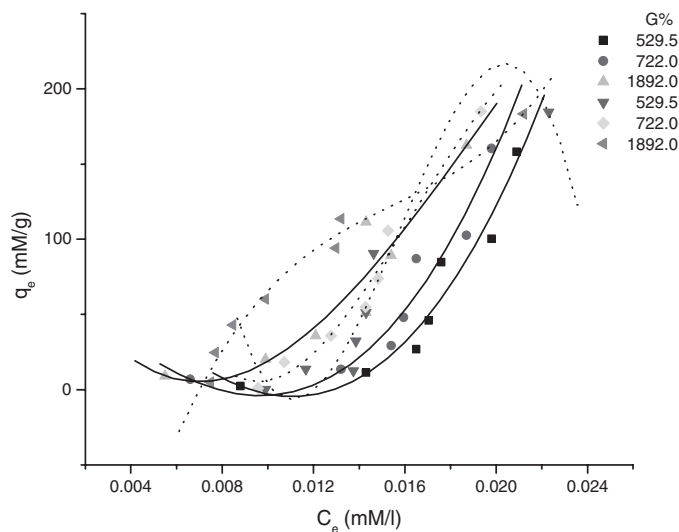

Fig. 10. Effect of concentration on adsorption capacity of Hg^{2+} onto PP-g-GMA (—) and after (. . . .) treatment at different initial solution concentrations of $Hg^{2+}$for PP-g-GMA before and after treatment, respectively at various grafting dose. Adsorption conditions: pH: 4.0 and 5.0 and I: 0.1 M KNO_3 at 25°C.
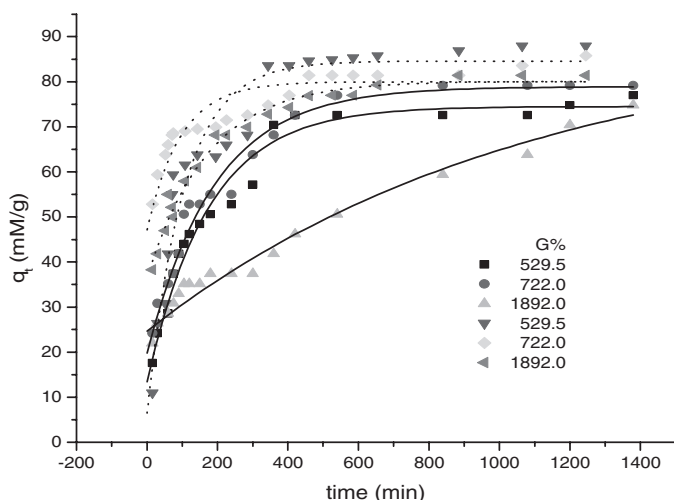

Fig. 11. Effect of contact time on the adsorption of Hg^{2+} onto PP-g-GMA before (—) and after (. . . .) treatment at various grafting dose. Adsorption conditions: pH: 4.0 and 5.0 for PP-g-GMA before and after treatment, respectively, and I: 0.1 M KNO_3 at 25°C.
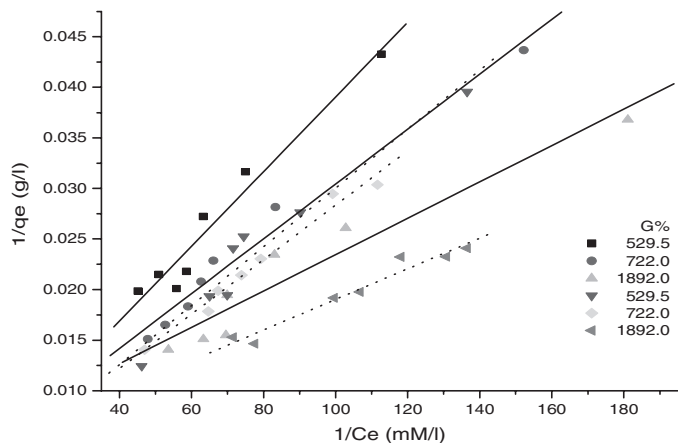
Fig. 12. Langmuir plot for adsorption of Hg^{2+} onto PP-g-GMA films before (—) and after (. . . .) treatment at various grafting dose. Adsorption condition: pH: 4.0 and 5.0 for PP-g-GMA before and after treatment, respectively, I: 0.1 M KNO_3 at 25°C.

Fig. 13. Freundlich plot for adsorption of Hg^{2+} onto PP-g-GMA films before (—) and after (. . . .) treatment at various grafting dose. Adsorption condition: pH: 4.0 and 5.0 for PP-g-GMA before and after treatment, respectively, I: 0.1 M KNO_3 at 25°C.
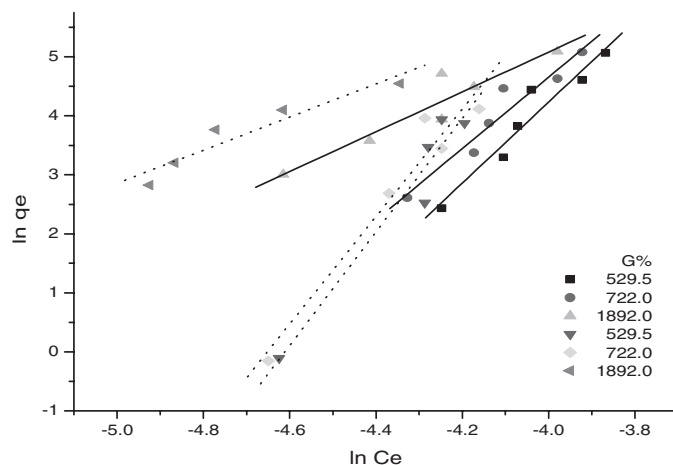
or unfavorable in batch processes defined by (37).

$$R_L = 1/(1 + K_L C_0) \quad (3)$$

where K_L is the Langmuir constant, C_0 the initial dye concentration (mg/L), R_L values indicate the type of isotherm to be irreversible ($R_L = 0$), favorable ($0 < R_L < 1$), linear ($R_L = 1$) or unfavorable ($R_L > 1$) (39,40). The K_L, Q_0 and R_L values for the adsorption of Hg^{2+} onto PP-g-GMA copolymers are given in Table 2.

Moreover, the Freundlich isotherm most widely used mathematical model, gives an empirical expression encompassing the surface heterogeneity and exponential distribution of active sites and their energy was tested in the following form (41).

$$q_e = K_F C_e^{1/n} \quad (4)$$

where K_F is adsorption capacity at unit concentration and $1/n$ is adsorption intensity. Equation) can be rearranged to a linear form (41).

$$\ln q_e = \ln K_F + 1/n \ln C_e \quad (5)$$

The $\ln K_F$ and $1/n$ values for the Freundlich adsorption isotherm (Figure 13) are listed in Table 2. As can be observed in Table 2, the higher correlation coefficients indicate

that there is a strong positive relationship for the data and that all experimental sorption data are better fitted to the Langmuir model. However, Freundlich model data are not in as good agreement as for the case of the Langmuir model. Moreover, according to Kadirvelu and Namasivayam (42), it has been shown that n values between 1 and 10 represent beneficial adsorption. Although both Langmuir and Freundlich model approximations of the observed adsorption data in the linearized forms give satisfactory correlation coefficients for most of the covered concentration range, the greater conformity of the adsorption data to the Langmuir isotherm (correlation coefficient > 0.98) implies that the sorption of metal ions on the PP-g-GMA follows the Langmuir isotherm. Consequently, it can be concluded that the metal ions adsorbed by the PP-g-GMA are adsorbed either in a monolayer or as a one-directional process; the Langmuir model is more suitable for analysis (43).

3.5 Kinetic Modeling

Most sorption processes take place by a multi-step mechanism comprising: (i) diffusion across the liquid film

Table 2. Langmuir and Freundlich constants for the adsorption of Hg^{2+} onto PP-g-GMA before and after treatments.

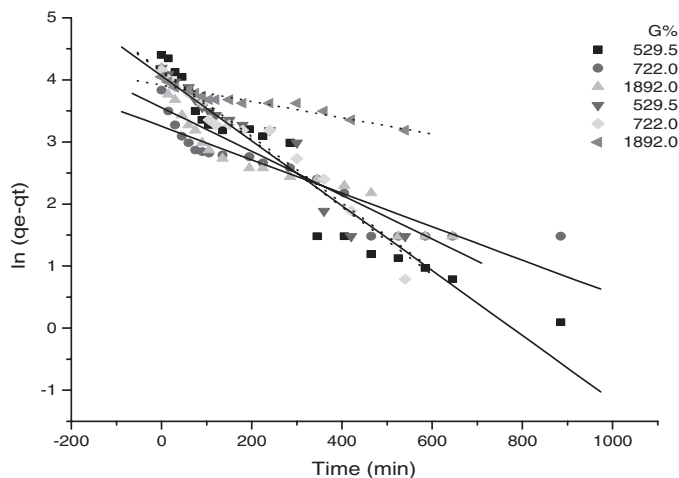|	Before							After						
	Langmuir				Freundlich			Langmuir				Freundlich		
G%	K_L	Q_0	r	R_L	$logK_F$	n	r	K_L	Q_0	r	R_L	$logK_F$	n	r
529.5	6.1	507.6	0.98	0.036	44.3	0.10	0.96	129.5	60.4	0.98	0.041	31.7	0.15	0.96
722.0	28.3	228.3	0.99	0.031	42.3	0.11	0.96	34.9	172.7	0.99	0.032	8.8	0.16	0.96
1892.0	9.7	769.1	0.96	0.031	16.8	0.04	0.94	27.9	230.3	0.98	0.045	18.5	0.29	0.94

Fig. 14. Pseudo-first-order kinetic plot for sorption of Hg^{2+} onto PP-g-GMA films before (—) and after (. . . .) treatment at various grafting percent. Adsorption condition: pH: 4.0 and 5.0 for PP-g-GMA before and after treatment, respectively, I: 0.1 M KNO_3 at 25°C.

Fig. 15. Pseudo-Second-order kinetic plot for sorption of Hg^{2+} onto PP-g-GMA films before (—) and after (. . . .) treatment at various grafting dose. Adsorption condition: pH: 4.0 and 5.0 for PP-g-GMA before and after treatment, respectively, I: 0.1 M KNO_3 at 25°C.
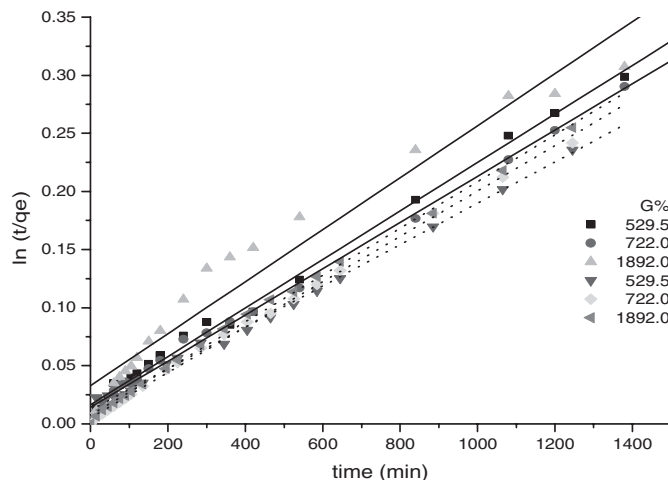
surrounding the solid particles (a process controlled by an external mass transfer coefficient), (ii) diffusion within the particle itself assuming a pore diffusion mechanism (intra-particle diffusion) and (iii) physical or chemical adsorption at a site (3.25). The transient behavior of the batch sorption process was analyzed using the Lagergren first-order kinetic model and the pseudo-second-order model (44–46).

In order to investigate the mechanism of sorption and potential rate-controlling steps such as mass transport and chemical reaction processes for Hg^{2+} onto pp-g-M, several kinetic models were tested including a pseudo-first- and pseudo-second-order equation. The transient behavior of the batch sorption process was analyzed using the Lagergren pseudo-first-order kinetic model (47–60). The Lagergren first-order model was given by the following differential equation:

$$(dq_t/dt) = k_1(q_1 - q_t) \tag{6}$$

After integration by applying the boundary conditions $q_t = 0$ at $t = 0$ and $q_t = q_t$ at $t = t$, Equation 5 becomes:

$$\ln(q_1/(q_1 - q_t)) = k_1t \tag{7}$$

Equation 6 can be rearranged to obtain a linear form:

$$\ln(q_1 - q_t) = \ln q_1 - k_1t \tag{8}$$

where q_1 and q_t are the amounts of Hg^{2+} sorbed at equilibrium and at time $t(mM/g)$, respectively, and k_1 is the equilibrium rate constant of pseudo-first-order sorption (l/min).

Moreover, the rate constant for pseudo-second-order sorption may be obtained from the following analysis(50, 51–53, 56, 61).

$$dq_t/dt = k_2(q_2 - q_t)^2 \tag{9}$$

Separating the variables in Equation 8 gives:

$$dq_t/(q_2 - q_t) = k_2t \tag{10}$$

Table 3. Comparison of the pseudo second- and first- order adsorption rate constants for Hg2+ onto PP-g-GMA before and after treatment.

	Before						After					
	Second order			First order			Second order			First order		
G%	$k_2 \times 10^4$	r	q_2	$k_1 \times 10^2$	r	q_1	$k_2 \times 10^4$	r	q_2	$k_1 \times 10^2$	r	q_1
529.5	73.94	0.98	99.8	2.60	0.97	82.2	94.53	0.99	104.31	1.18	0.96	95.0
722.0	5.04	0.99	81.7	1.76	0.93	65.1	6.39	0.99	82.90	1.82	0.92	44.2
1892.0	6.9	0.99	68.4	2.99	0.98	75.3	15.11	0.99	74.68	1.36	0.80	49.3

Integrating Equation 9 for the boundary conditions t = 0 to t = t and $q_t = 0$ to $q_t = q_t$, gives:

$$1/(q_2 - q_t) = 1/q_t + k_2 t \qquad (11)$$

where k_2 is the equilibrium rate constant of pseudo-second order sorption (g/mM min). Equation 10 can be rearranged to obtain a linear form (52).

$$t/q_t = (1/(k_2 q_2^2)) + (1/q_2)t \qquad (12)$$

and

$$h = k_2 q_2^2 \qquad (13)$$

where h is the initial sorption rate (mM/g min).

Figure 14 shows the fitted curves of Hg^{2+} at 30°C based on Equation 3. From Figure 14, it is observed that the sorption data are well represented by the Lagergren model only for the first 80 and 150 mins. for Hg^{2+} before and after treatment, respectively and thereafter it deviates from theory. This confirms that it is not appropriate to use the Lagergren kinetic model to predict the sorption kinetics of Hg^{2+} onto the PP-g-GMA for the entire sorption period. The predicted rate constants using the Lagergren equation from Figure 14 and its corresponding regression correlation coefficient values are shown in Table 3. As seen from the coefficients, data are less than 0.96 and the equilibrium capacities are lower comparing with the experimental data.

Moreover, Figure 15 presents the linear correlation of the pseudo-second-order kinetics for Hg^{2+}. In this study, the kinetic data shows good compliance with this pseudo-second-order equation (r>0.970). For the second-order kinetic rate (Table 3), after treatment it has a higher value than before.

Hence, this study suggested that the pseudo-second-order kinetic model better represented the adsorption kinetics, suggesting that the adsorption process might be chemisorptions. It is more likely to predict that the adsorption behavior may involve valence forces through the sharing of electrons between Hg^{2+} ions and adsorbent.

3.5.1. *Determination of the mercuryaffinity towered the grafted PP films using (EDX) analysis*

The adsorption selectivity is an indispensable factor for appreciating the capacities of an adsorbent. With this property, the PP grafted films can be used to adsorb a specific metal ion or separate specific metal ions from a solution contain specific metal ions. Figure 16 show the results of adsorption of metal ions onto poly PP-g-GMA at different grafting percent using a solution of Hg $^{+2}$ ions at pH 4.All investigation shows that the ratio of Hg^{+2} ion intensity increases as the degree of grafting increase which confirm that the high tendency and affinity of Hg^{+2} ions towards pp-g-GMA with functional groups of the grafted and treated pp films which forms more stable and strong complex.
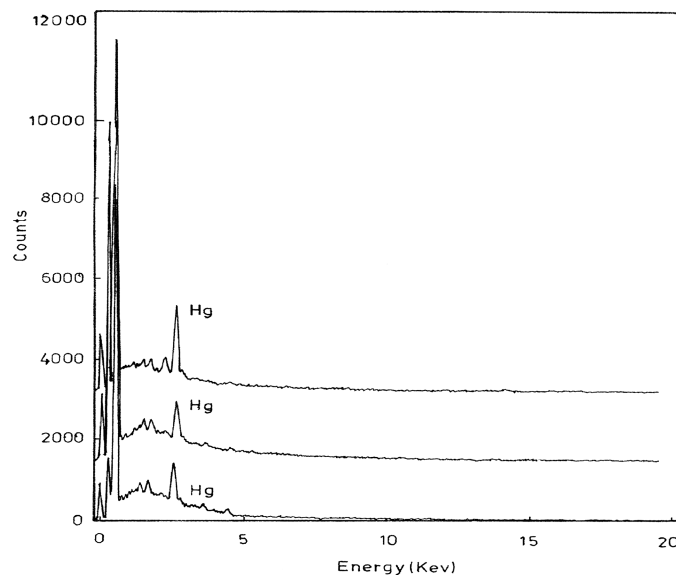

Fig. 16. EDX thermogram of PP-g-GMA with different grafting percent and carry Hg^{2+} metal ions.

4 Conclusions

The present study reveals that the polypropylene (PP) films grafted with glycidylmethacrelate (GMA) can be employed as an efficient adsorbent for the adsorption of Hg^{2+} from aqueous solutions. The efficiency of the grafted films increases by the chemical treatment to convert epoxy groups into amine groups. FT-IR, TGA, SEM and XRD data confirmed the efficient characterization and modification of PP-g-GMA. The batch experimental results show that PP-g-GMA, treated could be used for the direct removal of Hg^{2+} from aqueous solutions. The experimental data were analyzed in terms of Langmuir and Freundlich isotherm models and the data was well fit and more predominate to be applied by the Langmuir isotherm model the Freundlish isotherm model. The kinetic data correlated well with the pseudo-second-order kinetic model conformed that the adsorption process was by chemisorptions.

References

1. Inbaraj, B.S. and Sulochana, N. (2006) *Journal of Hazardous Materials*, B133, 283–290.
2. Green-Ruiz, C. (2006) *Bioresource Technology*, 97, 1907–1911.
3. Brigatti, M.F., Colonna, S., Malferrari, D., Medici, L. and Poppi, L. (2005) *Applied Clay Science*, 28, 1– 8.
4. Manohar, D.M., Anoop-Krishnan K. and Anirudhan, T.S. (2002) *Water Res.,* 36, 1609–1619.
5. Morel, F.M.M., Kraepiel, A.M.L. and Amyot, M. (1998) *Annu. Rev. Ecol. Syst.*, 29, 543–566.
6. Boening, D.W. (2000) *Chemosphere*, 40, 1335–1351.
7. Li, Nan, Bai, and Renbi. (2005) *Separation and Purification Technology*, 42, 237–247.

8. Ng, J.C.Y., Cheung, W.H. and McKay, G.J. (2002) *Colloid Interface Sci.*, 255, 64.

9. Bayrammoglu, G., Denizli, A., Sektas, S. and Arica, M.Y. (2002) *Microchem. J.,* 72, 63.

10. Doker, S., Malci, S., Dogan, M. and Salih, B. (2005) *Anal. Chim. Acta*, 5553, 73.

11. Ramesh, A., Hasegawa, H., Maki, T. and Ueda, K. (2007) *Separation and Purification Technology*, 56, 90.

12. Naguib, H.F., Aly, R.O., Sabaa, M.W. and Mokhtar, S.M. (2003) *Polymer Testing*, 22, 825–830, and references there in.

13. Nitto, K., Suzuki, S.I., Miyasaka, K. and Ishikawa, K. (1982) *J. Appl. Polym. Sci.*, 27, 637.

14. Mokhtar, S.M. and Sabaa, M.W. (1997) *Polym. Int.,* 42, 340.

15. Mokhtar, S.M. and Mostafa, T.B. (2000) *J. Polym. Res.*, 7, 215.

16. Odian, G., Acker, T. and Sobel, M. (1963) *J. Appl. Polym. Sci.*, 7, 245.

17. Mukherjee, A.K. and Gupta, B.D. (1985) *J. Appl. Polym. Sci.*, 30, 2235.

18. J. P. Wang, Y. Z. Chen, X.W. Ge and H. Q. Yu, Chemosphere, 66, (2007) 1752–1757.

19. Chiang, W.Y. and Huang, G.G. (1993) *J. Polym. Sci.*, 31, 381.

20. Maziad, N.A., Sayed, M.S. and Hegazy, E.A. (2002) *Poly. Int.,* 51, 150.

21. Nho, Y.C., Park, J.S. and Jin, J.H. (1997) *Pure Appl. Chem.*, A34, 831.

22. Choi, S.H., Nho, Y.C. and Kim, G.T. (1999) *J. Appl. Polym. Sci.*, 71, 643–650.

23. Sen, M., Pekel, N. and Güven, O. (1998) *Angew. Macromol. Chem.*, 251. 1.

24. El-Sawy, N.M., Hegazy, E.A., Rabie, A.A.M., Hamed, A. and Miligy, G.A. (1993) *Polym. Int*., 32, 131.

25. Deratani, A. and Sebille, B. (1981) *Macromol. Chem*., 182, 1875.

26. Merdivan, M., Karipcin, F. and Aggum, R.S. (1999) *J. Therm. Colorim.*, 58, 551.

27. Mitali, S., Pradip, K.A. and Bhaskar, B. (2003) *J. of Colloid and Interface Science*, 266, 28–32.

28. Sonmez , H.B., Senkel, B.F., Sherrington, D.C. and Bicak, N. (2003) *Reactive and Functional Polymers*, 55, 1.

29. Atia, A.A. (2005) *Hydrometallurgy*, 80, 13.

30. Chiou, M.S. and Li, H.Y. (2002) *Journal of Hazardous Materials,* B93, 233–248.

31. Jeon, C. and Holl, W.H. (2003) *Water Research*, 37, 4770.

32. Langmuir, I. (1918) *J. Am. Chem. Soc.*, 40, 1361–1368.

33. Freundlich, H.Z. (1906) *Phys. Chem.*, 57, 387–470.

34. Alley, E.R. Water Quality Control Handbook, 8, McGraw Hill: New York, 125, 2000.

35. Woodard, F. Industrial Waste Treatment Handbook, Butterworth-Heinemann, Boston, MA, 376, 2001.

36. Benefield, L.D., Judkins, J.F. and Weand, B.L. Process Chemistry for Water and Wastewater Treatment, Prentice-Hall, Inc.: Englewood, NJ, 191, 1982.

37. Longhinotti, E., Pozza, F., Furlan, L., Sanchez, M.N.M., Klug, M., Laranjeira, M.C.M. and Favere, V.T. (1998) *J. Braz. Chem. Soc.*, 9, 435.

38. Kinniburgh, G.D. (1986) *Environ. Sci. Technol.*, 20, 895.

39. Arami, M., Yousefi Limaee, N., Mahmoodi, N.M. and Salman Tabrizi, N. (2005) *J. Colloid. Inter. Sci*., 288, 371.

40. Sivaraj, R., Namasivayam, C. and Kadirvelu, K. (2001) *Waste Manag.,* 21, 105.

41. Rutheven; D.M. Principles of Adsorption and Adsorption Processes, Wiley: New York, 50, 1984.

42. Kadirvelu, K. and Namasivayam, C. (2000) *Environ. Technol.,* 21, 1091.

43. Jang, A., Seo, Y. and Bishop, P.L. *Environmental Pollution,* (2005) 133, 117.

44. Kumar, K.V., Ramamurthi, V. and Sivanesan, S. (2005) *J. Colloid Interface Sci.,* 284, 14.

45. Ho, Y.S. and McKay, G. (1998) *Process Saf. Environ. Prot.,* 76, 183.

46. Ho, Y.S. and McKay, G. (1999) *Process Biochem*., 34, 451.

47. Ho, Y.S. and Chiang, C.C. (2001) *Adsorption*, 7, 139.

48. Dogan, M. and Alkan, M. (2003) *Chemosphere,* 50, 517.

49. Ho, Y.S. and McKay, G. (1999) *Conservation Recycl.,* 25, 171.

50. Chiou, M.-S. and Li, H.-Y. (2002) *J. Hazard. Mater*., 93, 233.

51. Wu, F.-C., Tseng, R.-L. and Juang, R.-S. (2001) *Environ. Technol*., 22, 205.

52. Wu, F.-C., Tseng, R.-L. and Juang, R.-S. (2001) *Environ. Technol*., 22, 721.

53. Wu, F.-C., Tseng, R.-L. and Juang, R.-S. (2001) *Water Res.*, 35, 613.

54. Annadurai, G., Juang, R.-S. and Lee, D.-J. (2002) *J. Hazard. Mater.,* 92, 263.

55. Ozacar, M. and Sengil, I.A. (2002) *Adsorption*, 8, 301.

56. Ozacar, M. and Sengil, I.A. (2003) *J. Hazard. Mater.,* B98, 211.

57. Guo, Y., Yang, S., Fu, W., Qi, J., Li, R., Wang, Z. and Xu, H. (2003) *Dyes and Pigments*, 56, 219.

58. Ozacar, M. (2003) *Adsorption*, 9, 125.

59. Ozacar, M. (2003) *Chemosphere,* 51, 321.

60. Ozacar, M. (2003) *Cem. Concr. Res*,. 33, 1583.

61. Ho, Y.S. and Chiang, C.C. (2001) *Adsorption*, 7, 139.